Ionization of a Critical Adenosine Residue in the *Neurospora* Varkud Satellite Ribozyme Active Site†

Fatima D. Jones and Scott A. Strobel*

Department of Molecular Biophysics and Biochemistry and Department of Chemistry, Yale University, P.O. Box 208114, 260 Whitney Avenue, New Haven, Connecticut 06520-8114

Received December 20, 2002; Revised Manuscript Received February 12, 2003

ABSTRACT: The Varkud Satellite (VS) ribozyme catalyzes a site-specific self-cleavage reaction that generates 5′-OH and 2′,3′-cyclic phosphate products. Other ribozymes that perform an equivalent reaction appear to employ ionization of an active site residue, either to neutralize the negatively charged transition state or to act as a general acid−base catalyst. To test for important base ionization events in the VS ribozyme ligation reaction, we performed nucleotide analogue interference mapping (NAIM) with a series of ionization-sensitive adenosine and cytidine analogues. A756, a catalytically critical residue located within the VS active site, was the only nucleotide throughout the VS ribozyme that displayed the pH-dependent interference pattern characteristic of functional base ionization. We observed unique rescue of 8-azaadenosine (pK_a 2.2) and purine riboside (pK_a 2.1) interference at A756 at reduced reaction pH, suggestive of an ionization-specific effect. These results are consistent with protonation and/or deprotonation of A756 playing a direct role in the VS ribozyme reaction mechanism. In addition, NAIM experiments identified several functional groups within the RNA that play important roles in ribozyme folding and/or catalysis. These include residues in helix II, helix VI (730 loop), the II−III−VI and III−IV−V helix junctions, and loop V.

The *Neurospora* Varkud Satellite (VS)[1] ribozyme is a naturally occurring self-cleaving RNA found in the mitochondria of certain isolates of the species *Neurospora crassa* (*1*). It catalyzes a reversible self-cleavage reaction that generates 5′-OH and 2′,3′-cyclic phosphate products (*2*). The reaction involves nucleophilic attack of the scissile phosphate by the neighboring 2′-oxygen and displacement of the 5′-oxygen. An internal equilibrium between cleaved and ligated forms of the VS RNA may be important for the VS RNA replication cycle, where site-specific self-cleavage reactions generate monomeric and multimeric forms of the RNA that are subsequently self-ligated to generate closed circular VS RNA, the dominant form observed in vivo (*2*).

The active structure of the VS ribozyme is contained within 154 nucleotides that fold into six helices (I−VI) (*3*). A seventh helical element (VII), formed by complementary nucleotides 5′ of the cleavage site and 3′ of the ribozyme sequence, is important for the ligation activity of the RNA (*4*). In addition to the seven helical elements, a three base pair kissing interaction is formed between the loops at the ends of helices I and V (*5*, *6*). Formation of this tertiary contact induces a pH-dependent shifted base pairing alignment within the substrate helix (stem−loop I) that is required for activity (*7*, *8*).

Mutational studies show that the 730 loop, an asymmetric bulge within helix VI, is a critical component of the ribozyme active site (*9*). Though much of the sequence in helix VI is expendable for self-cleavage, deletion, mutation, or analogue substitution of nucleotides in the 730 loop severely impairs self-cleavage activity in vitro (*10*−*13*). Of particular importance is nucleotide A756, which is the nucleotide most sensitive to mutation or modification. Substituting A756 with any base (C, G, or U) results in catalytic rate reductions greater than 300-fold (*10*, *11*). Deletion or modification of the base significantly reduces the catalytic rate (>900-fold), though removal of the 2′-OH group from A756 reduces the rate of cleavage only 10-fold (*13*). While mutation of A756 reduces the reaction rate, it does not appear to affect folding or substrate binding (*10*). These results suggest an important catalytic role for A756 in VS RNA activity.

A high-resolution crystal structure for the VS ribozyme is not yet available, but other biophysical approaches have provided valuable structural insight. Using FRET measurements to determine the orientation of the II−III−VI and III−IV−V helical junctions, Lafontaine et al. modeled the global architecture of the VS ribozyme (*14*). In their model, the substrate helix (stem−loop I) docks into a cleft formed by helices II and VI. In this orientation, the cleavage site makes

† This work supported by a National Research Service Award (NIH) to F.D.J. and by an NSF grant CHE-0100057 to S.A.S.

* Corresponding author. E-mail: strobel@csb.yale.edu. Phone: (203) 432-9772. Fax: (203) 432-5767.

[1] Abbreviations: A, adenosine; dA, 2′-deoxyadenosine; 7dA, 7-deazaadenosine; Pur, purine riboside; DAP, 2,6-diaminopurine riboside; 2AP, 2-aminopurine riboside; n^8A, 8-azaadenosine; FormA, formycin A; C, cytidine; dC, 2′-deoxycytidine; n^6C, 6-azacytidine; f^5C, 5-flourocytidine; ΨiC, pseudoisocytidine; G, guanosine; dG, 2′-deoxyguanosine; U, uridine; dU, 2′-deoxyuridine; NAIM, nucleotide analogue interference mapping; VS, varkud satellite; FRET, fluorescence resonance energy transfer.

10.1021/bi020707t CCC: $25.00
Published on Web 03/21/2003

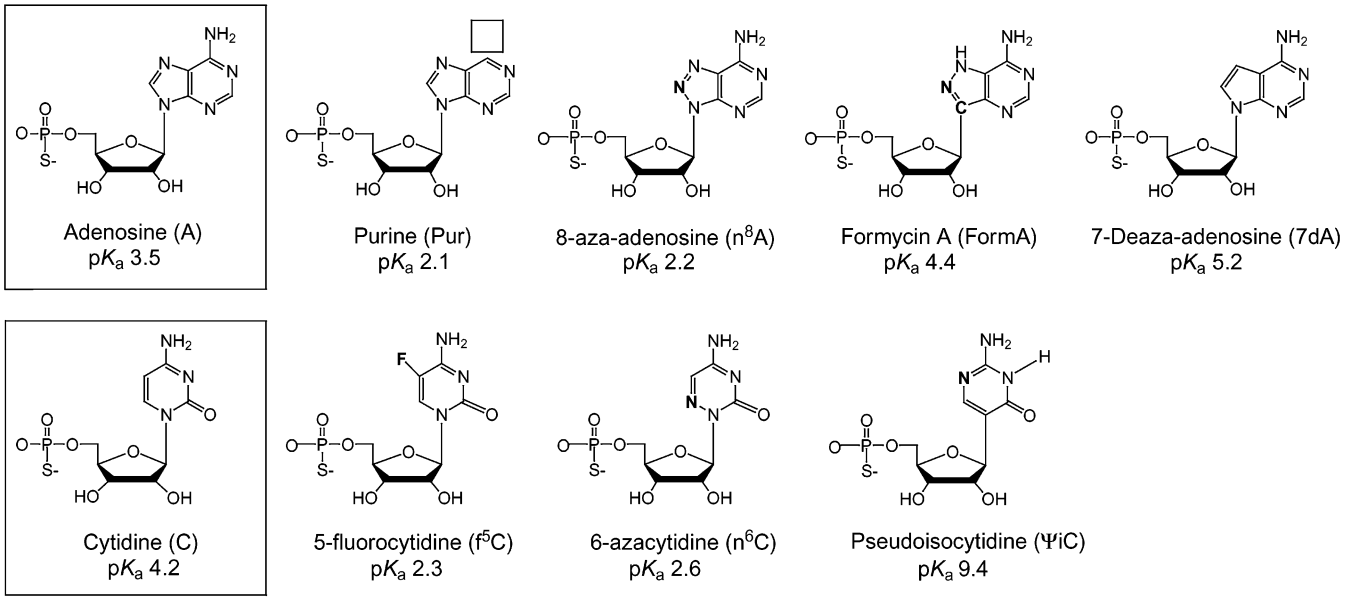

FIGURE 1: pK_a-shifted adenosine and cytidine nucleotide analogues used in pH-dependent NAIM analysis. The name, abbreviation, and pK_a of each nucleoside is indicated. The chemical change from adenosine or cytidine for each analogue is indicated in bold or is boxed. The indicated pK_as are for the free nucleosides. The unperturbed pK_as for the nucleotides are likely to be about 0.5 pH unit higher due to the 3′- and 5′-phosphate groups (*38*, *39*).

tertiary contacts with nucleotides in the 730 loop. Consistent with such a helical packing alignment, cross-linking experiments with 4-thiouridine demonstrated a direct contact between A756 and the cleavage site of the substrate helix (*15*).

While the chemical reaction promoted by the VS ribozyme is known, the mechanism of its catalysis remains an open question. It was initially assumed to be a metalloenzyme, but it was subsequently found to react efficiently in the absence of divalent metal ions (*16*). This argues against a mechanism of metal ion-mediated catalysis. An alternative possibility is a proton transfer mechanism, such as general acid or general base catalysis, but the lack of pH dependence on the reaction rate argues against this hypothesis (*17*). However, the pH dependence data may be misleading. A pH-independent step other than chemistry may be rate limiting, such as formation of the kissing interaction, which would serve to mask the pH dependence of the chemical step (*6*, *7*). Alternatively, a pH-independent reaction profile may also reflect multiple ionization events in opposite directions that cancel out to yield a net pH independence.

Other catalytic RNAs, which perform phosphotransfer reactions equivalent to that of the VS ribozyme, are proposed to utilize a general acid−base mechanism involving ionization of active site residues (*18*−*20*). It is possible that the VS ribozyme may also employ an ionized base to facilitate catalysis, but there is little or no evidence in support of this hypothesis. To explore this possibility, we employed a series of adenosine and cytidine analogues with N1- and N3-perturbed pK_a values, respectively, in nucleotide analogue interference mapping (NAIM). These analogues make it possible to simultaneously, yet individually, assay for functionally important base ionization at every A or C residue in an RNA. Each of the analogues is prepared as a triphosphate for transcriptional incorporation into an RNA and tagged with an α-phosphorothioate linkage, a bond that can be cleaved with iodine to reveal the position of analogue incorporation within the RNA polymer. These analogues were instrumental in the identification of a protonated C (C300) important for folding of group I introns, ionization of a C (C75) in the active site of the genomic HDV ribozyme, and the ionization of an A (A10) in the active site of the hairpin ribozyme (*18*, *21*, *22*). They are ideally suited to assay for base ionization within the VS ribozyme.

Four adenosine analogues are useful in the detection of adenosine ionization by NAIM, namely, 8-azaadenosine (n^8A), formycin A (FormA), purine riboside (Pur), and 7-deazaadenosine (7dA) (Figure 1). n^8A has an additional nitrogen in the five-membered ring that reduces the N1 pK_a in the six-membered ring to 2.2, compared to the pK_a of 3.5 for A (*23*). FormA is a C-linked nucleotide that, like n^8A, has an N8 imino group, but the pK_a of the N1 group is increased to 4.4 (*24*). As a result FormA can be used to control for deleterious effects resulting from the N8 substitution. Pur is an adenosine analogue that lacks the N6 exocyclic amine. As a result, Pur is typically used to identify hydrogen-bonding contacts to the major groove face of the base; however, Pur, like n^8A, has a reduced N1 pK_a of 2.1. Thus, Pur interference is ambiguous. It may result from either the absence of the N6 amine or the reduced pK_a of the base (or both). 7dA lacks the N7 imino group and has an increased pK_a of 5.2 (*25*). Interference by 7dA suggests interactions to the N7 imino group of A; however, due to the elevated pK_a of the base, enhancement may be observed at sites of ionization.

On the basis of previous studies with these analogues (*18*), the following interference pattern is expected at individual adenosine residues whose ionization is functionally important. At elevated pH, interference is observed with both Pur and n^8A. The interference is at least partially rescued by lowering the pH of the buffer. Furthermore, enhanced activity may be observed with FormA or 7dA at sites of base ionization due to the increased basicity of these nucleotides,

if base ionization is a limiting event in the reaction.

Similar to the adenosine analogue series, we have utilized three cytidine analogues to assay for positions of cytidine ionization, namely, 6-azacytidine (n^6C), 5-fluorocytidine (f^5C), and pseudoisocytidine (ΨiC) (Figure 1). In n^6C, substitution of the pyrimidine C6 with nitrogen lowers the pK_a of the N3 from 4.2 to 2.6. Similarly, replacing the C5 hydrogen with fluorine in f^5C reduces the N3 pK_a to 2.3. At those positions where N3 ionization of C within the RNA is important for activity, both n^6C and f^5C have been shown to cause interference at high pH due to the increased acidity of both analogues. But as is the case for the adenosine analogues, the interference is also pH dependent. ΨiC is a C-linked nucleotide with enhanced basicity at N3, resulting in an N3 pK_a of 9.4. ΨiC can adopt two tautomeric forms with the proton on either the N1 or the N3 position. The N3 tautomer is the slightly more stable of the two, which makes it effectively a protonated cytidine analogue at neutral pH, without the requirement for ionization. As a result, ΨiC incorporation results in pH-dependent enhancement at sites where N3 protonation is required for hydrogen bonding, as was observed within the C^+·G·C base triple of the *Tetrahymena* group I intron (*21*, *26*).

Here we report the use of these pK_a-perturbed adenosine and cytidine analogues to assess the requirement for base ionization in the VS reaction. On the basis of the interference pattern and its pH dependence, ionization of A756, the critical nucleotide located within the active site, appears to be important for the ligation activity of the VS ribozyme. The possible roles that A756 protonation may play in VS activity are discussed.

MATERIALS AND METHODS

DNA Templates and RNA Synthesis. NAIM experiments were performed with the VSE ribozyme construct (Figure 2) previously reported (*4*). This RNA contains two mutations, A782U and U785C, in the extended helical element (helix VII) that enhance ligation activity in vitro. VSE RNA was prepared by transcription from *Ear*I-cut plasmid pHHVS, which encodes the hammerhead ribozyme sequence upstream of the VS cleavage site. Processing of the hammerhead ribozyme during or after transcription generates the full-length cleaved form of VSE RNA with a hydroxyl at the 5′-end, which is the chemical form required for ligation. Transcription reactions contained 40 mM Tris-HCl (pH 8.0), 10 mM $MgCl_2$, 2 mM spermidine, 5 mM DTT, 0.005% Triton X-100, 1 mM each NTP, and either T7 polymerase or the mutant polymerase Y639F. Y639F was used to incorporate analogues with substitutions at the 2′ position. Random incorporation of the nucleotide analogues was achieved by including in the transcription reaction the empirically determined concentration of the nucleotide analogue necessary to obtain approximately 5% incorporation (*18*, *21*, *27*, *28*). However, Pur and n^8A were incorporated at final concentrations of 4 and 0.8 mM, respectively, which is higher than the reported value but was necessary to achieve efficient incorporation in this transcript. VS RNAs were purified by 8% denaturing PAGE and eluted in 10 mM Tris-HCl (pH 8.0), 0.1 mM EDTA, 250 mM NaCl, and 2% sodium dodecyl sulfate (SDS) for 30 min at room temperature. RNAs were extracted with 1 volume of phenol−chloroform−isoamyl alcohol (PCA), concentrated by ethanol precipitation, and resuspended in TE (10 mM Tris-HCl, 0.1 mM EDTA, pH 8.0). Addition of SDS and shortened elution times were required to minimize the degradation of the RNA, particularly in the A756 region. RNA transcripts were stored at −80 °C until use. 5′-End-labeled substrate RNA (SUB24) was prepared as previously described (*4*).

NAIM Analysis of the VS Ribozyme Ligation Reaction. VS RNAs containing randomly incorporated nucleotide analogues were assayed for the ability to ligate a 5′-end-labeled substrate RNA (SUB24). Interference experiments were performed at 30 °C in 25 mM KCl, 5 mM $MgCl_2$, and 50 mM buffer ranging from pH 5.4 to pH 8.0. In some cases multiple buffers were used to control for buffer-specific effects. All of the buffers were used within 1 pH unit of their reported pK_a: potassium acetate (pH 5.4), MES (pH 5.4), MOPS (pH 6.0 and 6.5), HEPES (pH 7.0 and 8.0), and Tris-HCl (pH 7.0 and 8.0). The ribozyme (0.4 μM) was incubated in buffer at 50 °C for 15 min, slow cooled, and incubated at 30 °C for an additional 5 min. Ligation reactions were initiated by addition of prewarmed 5′-end-labeled substrate RNA (SUB24, ∼0.1 μM) and incubated at 30 °C for a time sufficient to obtain approximately 6% ligation. Upon ligation with this substrate, the ribozyme becomes labeled at its 5′-end. Incubation times were extended at low pH to normalize for the extent of reaction: pH 8.0 and 7.0 (20 min), pH 6.0 (30 min), pH 5.5 (60 min), and pH 5.4 (80 min). Reactions were quenched by the addition of one volume of formamide loading buffer (FLB), cleaved with $^1/_{10}$th volume of 100 mM iodine, and heated at 90 °C for 2 min. Cleavage products were resolved on an 8% denaturing polyacrylamide gel to reveal the sites of analogue substitution and interference. Reactions not treated with iodine were also prepared to control for nonspecific background degradation. Unselected transcripts radiolabeled at their 5′-ends were prepared to control for the extent of analogue incorporation at each site (see 5′-controls, Figure 4B). The transcripts were labeled using T4 polynucleotide kinase and [γ-^{32}P]ATP. Labeled RNAs were eluted in crush−soak buffer (10 mM Tris-HCl, 0.1 mM EDTA, 250 mM NaCl) and 2% SDS, PCA extracted, ethanol precipitated, and resuspended directly in FLB. RNAs were treated with iodine as above and resolved on a denaturing acrylamide gel.

Interferences or enhancements are denoted by reduced or increased intensity of the band in the gel, respectively, relative to the unselected 5′-end-labeled control. Interference κ values were quantified as described by Ryder and Strobel (*28*). Individual band intensities for both the parental nucleotide (NαS) and nucleotide analogue (δαS) were quantitated by area integration using ImageQuant (Molecular Dynamics) software. The extent of interference at each position was calculated by substituting the individual band intensities into the equation:

$$\kappa = (\text{N}\alpha\text{S ligation}/\delta\alpha\text{S ligation})/(5'\text{N}\alpha\text{S control}/5'\delta\alpha\text{S control}) \quad (1)$$

where NαS ligation and δαS are the intensities of the phosphorothioate-tagged parental nucleotide and the analogue for the ligation reaction, respectively. 5′NαS control and 5′δαS control are the band intensities for the phosphorothioate-tagged parental nucleotide and the analogue in the

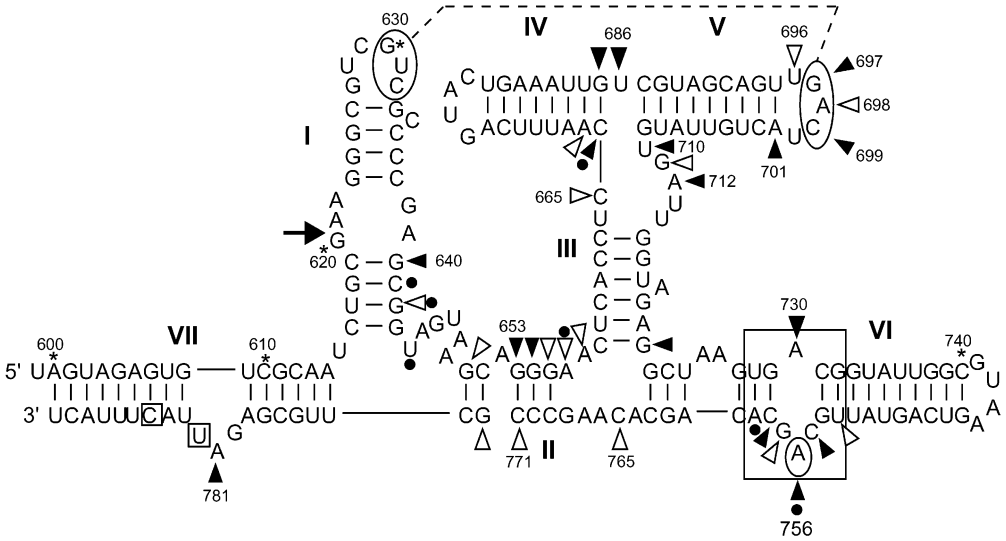

FIGURE 2: Secondary structure of the VS ribozyme ligation construct (VSE) used in NAIM analysis. The VSE construct contains two mutations in helix VII that enhance ligation activity (boxed nucleotides). Positions where analogue substitution interfered with activity are indicated with arrowheads. Filled arrowheads designate strong interferences from at least one of the analogues tested ($\kappa \geq 4.0$), while open arrowheads indicate moderate interferences ($2.5 < \kappa < 4.0$). Positions of enhancement ($\kappa \leq 0.5$) are indicated with a closed circle. Most positions in VS were informative, with the exception of nucleotides 621−639 and 782−791 that could not be resolved on a denaturing gel. The substrate (SUB24) used in these experiments included VS nucleotides 599−620, as shown. No information was obtained for residues 599−620 because analogues were not incorporated within this region. The kissing interaction (dashed line) and the position of the 730 loop (boxed region) are shown. The position of the critical nucleotide A756 is circled. The arrow to the left of helix I indicates the site of cleavage and ligation.

unselected 5′-end-labeled RNA, respectively. This calculation normalizes for both the extent of analogue incorporation and for interferences resulting from the phosphorothioate tag (*28*). On the basis of the level of noise in the interference analysis, κ values of 2 or greater are reliable indicators of interference, while κ values less than 0.5 indicate enhancement. A κ value of 1 indicates no interference. Maximal interference for this system was defined as having a κ value of 6.

RESULTS

Phosphorothioate and 2′-Deoxy Effects in the VS Ligation Assay. We employed a ligation-based NAIM assay using the self-ligation construct VSE (Figure 2) to probe important functional groups throughout the VS RNA. Of the 171 nucleotides in this construct, 142 nucleotides (G640-A781) were informative for the assay. The 29 exceptions are nucleotides at the 5′- or 3′-most ends of the ribozyme and those residing near the cleavage/ligation site, which were uninformative due to incomplete band resolution on the sequencing gels.

Previous work utilized NAIM to identify several phosphate and 2′-OH groups that play important functional roles in the VS ribozyme self-cleavage reaction (*29*, *30*). We first sought to determine if these same functional groups interfere with the ligation activity of the ribozyme. Toward this goal, we incorporated the four α-phosphorothioate-tagged parental nucleotides (A, C, G, and U) into the VS ligation construct and assayed for positions of (R_P)-phosphorothioate interference. Interference was observed at several sites within the RNA (Figure 3A). Strong effects ($\kappa \geq 4.0$) were detected at nucleotides G640, C755, and C758, while moderate effects ($4.0 > \kappa \geq 2.5$) were observed at nucleotides C699, G653, and G757. These are the same six residues previously reported to show interference in a self-cleavage assay (*29*). A few positions also showed modest phosphorothioate enhancements, including nucleotides C641, G642, C666, and A759 (Figure 3A). With the exception of nucleotides G642 and C666, all of the phosphorothioate effects observed in the ligation assay were equivalent to those reported for the self-cleavage assay (see Table 1) (*29*).

In addition to the parental phosphorothioate analogues, four α-phosphorothioate-tagged 2′-deoxynucleotide analogues (dA, dC, dG, and dU) were used to assay for positions in the RNA where the 2′-OH group is functionally important (Figure 3B). The range of informative residues was equivalent to that for the phosphorothioate series except for positions C755 and C758 that could not be assayed due to strong phosphorothioate effects. Residues that showed interference in both the cleavage and ligation assays are underlined. The strongest 2′-deoxy effects ($\kappa \geq 4.0$) were observed at six residues: G653, G654, U686, A701, U710, and A712. Moderate effects ($4.0 > \kappa \geq 2.5$) were observed at nucleotides G655, C666, A667, U696, A698, U753, A756, and C771 and weak effects ($2.5 > \kappa \geq 2.0$) at nucleotides U659, G697, U713, U752, and G754. Enhanced activity resulting from 2′-deoxynucleotide substitution was observed at nucleotides U644 and A656. The 2′-deoxy effects are largely, though not completely, consistent with those previously reported in the self-cleavage assay (see Table 1). Although reported in the self-cleavage assay (*30*), no significant 2′-deoxy effects were observed at positions C641, C699, G757, A759, A767, and C770 in the ligation assay. The minor discrepancies in the interference pattern may reflect subtle structural differences in the ligation and cleavage reactions, possibly resulting from the presence of helix VII, or differences in the sensitivity of the two assays. However, the overall similarity between these two data sets suggests that the two constructs assay for effects at similar steps in the reaction pathway.

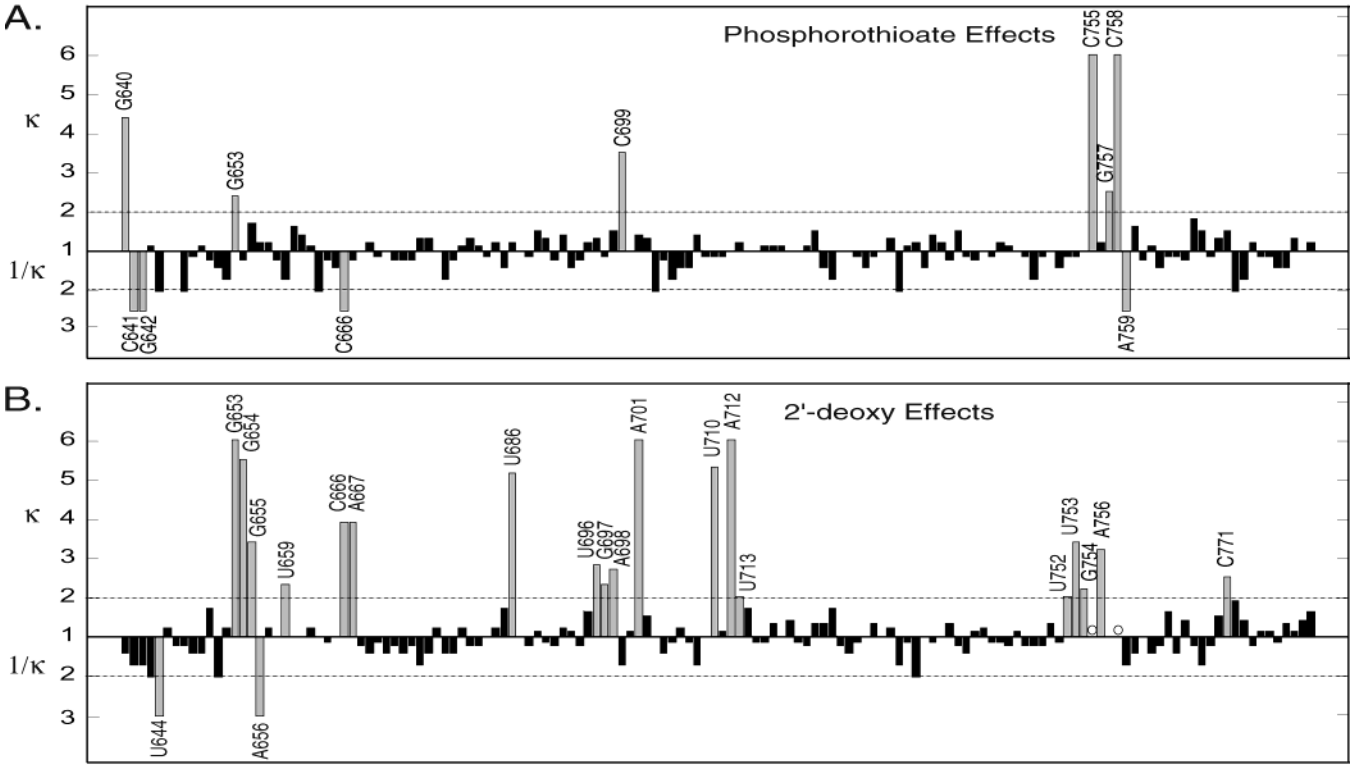

FIGURE 3: Phosphorothioate and 2′-deoxy interference results. The quantitated interference (κ) values for ligation reactions with parental phosphorothioate (A, C, G, and U) and 2′-deoxy (dA, dC, dG, and dU) nucleotide analogues at pH 7 are plotted for each nucleotide position in the VS ribozyme. Significant interferences ($\kappa > 2$) and enhancements ($\kappa < 0.5$) are indicated in gray shading, while those positions that do not significantly affect catalysis are indicated in black. Nucleotides C755 and C758 were uninformative in the 2′-deoxy assay due to strong phosphorothioate effects, as indicated by open circles. Maximal interference is indicated by a κ value of 6. κ values less than 1 are reported as $1/\kappa$, and the value is graphed below the center point.

Base-Modified Adenosine and Guanosine Analogues. We also performed NAIM analysis using a series of base-modified adenosine and guanosine analogues to assess contributions made by individual purine functional groups toward the activity of the VS ribozyme. Four adenosine analogues and three guanosine analogues were selected for the analysis. 7-Deazaadenosine (7dA) assesses contributions made by the N7 imino group, while 2,6-diaminopurine riboside (DAP) and 2-aminopurine riboside (2AP) are used to determine whether an N2 exocyclic amine can be accommodated in the minor groove. Interferences by both DAP and 2AP reveal positions where an A to G mutation is likely to be detrimental to function. Together, 2AP and Pur are used to evaluate the role of the N6 exocyclic amine. The guanosine analogues included 7-deazaguanosine (7dG), inosine (Ino), and N^2-methylguanosine (m^2G). 7dG reveals interactions to the N7 imino, while Ino and m^2G are useful in assessing the importance of the N2 amine of guanosine. The residues that showed the greatest level of interference are located in helix II, the III−IV−V helix junction, the kissing interaction, and the 730 loop in helix VI. All of these regions were previously shown to be important for catalysis (*6*, *9*, *10*, *14*). The residues that showed the most pronounced effects were G640 (Ino, m^2G), G653 (Ino, m^2G), G654 (7dG, Ino, m^2G), G697 (7dG, Ino), A698 (7dA, Pur), A701 (7dA, DAP, 2AP, Pur), A712 (7dA, DAP, 2AP), A730 (DAP, 2AP), and A756 (7dA, DAP, 2AP, Pur); see Figures 4A and 5.

Without additional structural information or interference suppression analysis, it is not possible to unambiguously ascribe a cause to all of these interferences, though some of them are suggestive of important structural features in the active ribozyme. Several of the interferences cluster to nucleotides surrounding the helix I−helix V kissing interaction. For example, Pur interference at A698 and Ino interference at G697 are consistent with Watson−Crick base pairing to U631 and C632, respectively (*6*). Normally, Ino and Pur substitutions show interference in duplexes only when duplex stability is critical for ribozyme function (*31*). Other interferences at these two positions suggest that more than simple base pairing occurs in this region. 7dG interference at G697 and 7dA interference at A698 are suggestive of interactions in the major groove of the helix, indicating that additional tertiary contacts may stabilize the kissing interaction. Furthermore, strong DAP and 2AP interference at A701, the closing base pair in helix V, suggests that there is also close approach in the minor groove edge at the end of the helix.

A particularly interesting pattern of interference was observed within helix II. Strong Ino interference was observed at two consecutive nucleotides in the middle of helix II, residues G653 and G654 (Figure 5A). As was the case in the kissing interaction, this interference may result from the reduced base-pairing potential of Ino. As was mentioned previously, however, Ino interference is rarely seen within duplex regions. Instead, this pattern is more likely to result from a critical tertiary interaction in the helix II

Table 1: Comparison of the Self-Cleavage and Self-Ligation Interference Assays[a]

nucleotide position	phosphorothioate		2′-deoxyribonucleotide	
	cleavage[b]	ligation (κ)	cleavage[c]	ligation (κ)
G640	++	++		
C641	−	−	−	
G642		−		
U644			−	−
G653	++	++	++	+++
G654			++	+++
G655			++	++
A656				-
U659			+	+
C666		−	+	++
A667				++
U686			++	+++
U696			++	++
G697				+
A698			++	++
C699	++	++	++	
A701			+++	+++
U710			++	+++
A712			+++	+++
U713			+	+
U752				+
U753			+	++
G754			+	+
C755	+++	+++	+++	*
A756			++	++
G757	++	++	++	
C758	+++	+++	+++	*
A759	−	−	−	
A767			−	
C770			++	
C771			+++	++
G772			++	+

[a] Interference values reported as strong (+++, $\kappa > 4.0$), moderate (++, $4.0 < \kappa < 2.5$), weak (+, $\kappa < 2.5$), or enhancement (−, $\kappa < 0.5$). (*) Uninformative due to strong phosphorothioate effects. [b] Cleavage data adapted from Sood (*29*). [c] Cleavage data adapted from Sood (*30*).

minor groove. To further explore this possibility, we performed NAIM analysis with N^2-methylguanosine (m^2G). This analogue replaces one of the hydrogens of the N2 exocyclic amine of G with a methyl group. m^2G does not interfere at regions attributed to secondary structure stability (*32*); thus interferences with both Ino and m^2G are indicative of minor groove tertiary interactions (*33*). m^2G did not interfere with activity when incorporated at G697 in the kissing interaction, consistent with Ino interference resulting from reduced duplex stability (Figure 5A). However, strong m^2G interference ($\kappa > 5$, Figure 5A) was observed at nucleotides G653 and G654, which indicates that there are likely to be tertiary contacts at these two consecutive base pairs in helix II. In addition to the exocyclic amine, the 2′-OH groups of these two residues, as well as residue C771, are also important for activity. This interference pattern is characteristic of the receptor base pairs in an A-minor motif (*34*, *35*).

Nucleotide A756 was the most sensitive to modification of all the positions in the VS RNA. All of the adenosine analogues tested caused either interference (dA, DAP, Pur, and 2AP) or enhancement (7dA) when incorporated at this position (refer to Figures 4A and 5B). DAP and 2AP interference at A756 is consistent with previous reports that mutating A756 to G reduces self-cleavage activity more than 90-fold (*10*, *11*). Pur interference at A756 suggests that the N6 amine is important for activity; however, this interference could also result from the reduced pK_a of the purine base, and the 7dA enhancement may also result from base ionization.

pK_a-Perturbed Nucleotide Analogues. To further explore this possibility, we undertook a NAIM analysis using the pK_a-perturbed adenosine and cytidine analogues in an effort to identify positions of functionally important base ionization in the VS ribozyme. This analysis utilized the adenosine analogues n^8A, Pur, FormA, and 7dA and the cytidine analogues f^5C, n^6C, and ΨiC (Figure 1). As was mentioned previously, n^8A, like Pur, has an N1 pK_a shift, but unlike Pur, all of the adenosine functional groups are available for hydrogen bonding.

The interference pattern of the adenosine analogue series is consistent with base ionization of A756 during the ligation reaction. At pH 7, n^8A incorporation caused interference at three positions within the VS ribozyme: A712, A756, and A781 (Figures 4A and 5B). These interferences could result from the reduced pK_a of the nucleotide or the additional imino group in the five-membered ring. To control for interferences due to substitution at the N8 position, we assayed for FormA interferences. Two of the three sites of n^8A interference also showed FormA interference, namely, A712 and A781 (Figures 4A and 5B). A modest effect was also observed at A667. In contrast to these positions, FormA substitution at A756 resulted in enhanced ligation activity (see Figure 6A). Thus, FormA and 7dA have elevated pK_a values and both show enhancement at A756, and n^8A and Pur have reduced pK_a values and both show interference. This is consistent with ionization of A756 being important for the VS ligation reaction.

To further test if the interferences at A756 reflect base ionization, we performed the NAIM assays at pHs ranging from 8.0 to 5.4. At pH 5.4 several interferences were stronger than at pH 7.0, which suggests that the assay is more sensitive at the reduced pH (For example, see the pH data in Figure 7.) n^8A interference at A756 persisted at pH 7.0 and 6.0; however, at pH 5.4 the interference was essentially eliminated (Figure 6B). Similarly, the A756 Pur interference observed at pH 7.0 was rescued at pH 5.4 (Figure 6A). Thus, both of the pK_a-perturbed adenosine analogues demonstrated a pH-dependent interference pattern at A756. The specificity of the effect was tested using dA, an analogue that does not have a reduced pK_a but causes interference at A756. As predicted, dA interference at A756 was unaffected across the pH range, including pH 5.4 (Figure 6A). FormA enhancement at A756 was also unaffected by the reduced pH. Furthermore, the other sites of significant n^8A interference, A712 and A781, were not significantly altered as the pH was lowered (Figure 6B). The pH-dependent interference pattern at A756 was quantitated and is summarized in Figure 6C.

We also explored potential sites of cytidine ionization within the VS RNA using the pK_a-shifted cytidine analogues (Figure 1). The expectation for a functionally important ionized cytidine residue is that n^6C and f^5C would both show interference at a particular site because both have a similarly reduced pK_a. Within the VS RNA at pH 7, n^6C showed modest interference at three sites (C666, C760, and C765), but there were no interferences resulting from f^5C incorporation, nor were there any sites of ΨiC interference or

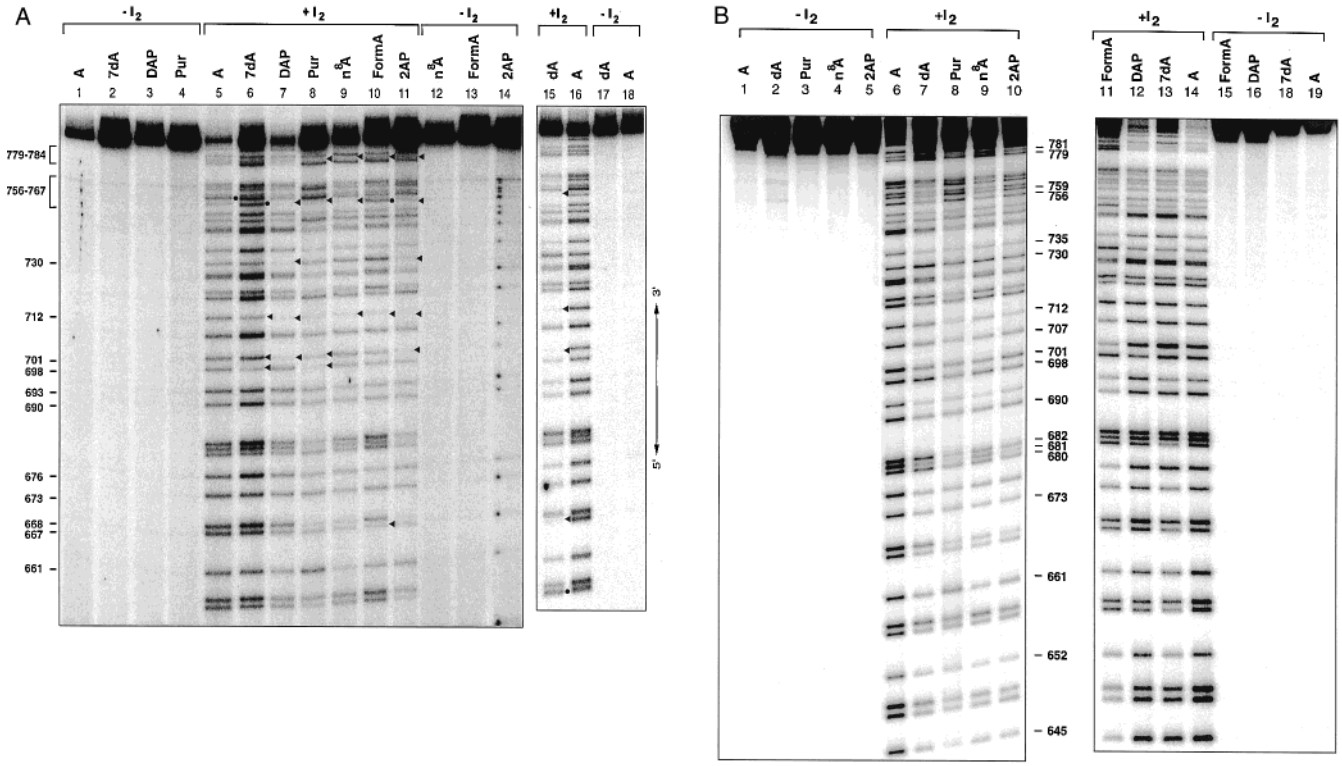

FIGURE 4: (A) NAIM ligation reactions with the adenosine analogues. Lanes 5−11 correspond to reactions with A, 7dA, DAP, Pur, n^8A, FormA, and 2AP. Reactions with dA are shown in lane 15. Iodine was not added to the RNA loaded into lanes 1−4, 12−14, 17, and 18. This controlled for nonspecific background degradation of the RNA. Sites of interference ($\kappa \geq 2.5$) are indicated by an arrowhead to the right of each lane, while sites of enhancement are indicated by a closed circle. Nucleotide positions are shown to the left of the gel. (B) Controls for extent of analogue incorporation at each position. Unselected RNAs containing analogue substitutions were 5′-radiolabeled, purified by denaturing gel electrophoresis, and treated with iodine (lanes 6−14) to reveal the extent of analogue incorporation at each site. No iodine controls (lanes 1−5 and 15−19) were also prepared to control for background degradation.

enhancement (see Figure 7). Furthermore, the n^6C interferences were not rescued by a reduction in the reaction pH (Figure 7). This suggests that the modest interference effects resulted from the 6-aza substitution rather than the alteration in the pK_a of the nucleotide. This trend is in marked contrast to the pH-dependent n^8A interference suppression at A756. Thus, after virtually every adenosine and cytidine residue in the VS RNA was assayed for base ionization, A756 is the only one that showed a pattern consistent with such an effect.

DISCUSSION

We performed NAIM using a VS ribozyme ligation assay to investigate the structural and functional properties of this RNA. NAIM experiments were performed using several base- and ribose-modified nucleotides, including the parent phosphorothioate derivatives and a series of pK_a-shifted analogues. Sites of phosphorothioate and 2′-deoxyribonucleotide interference correlated well with those previously reported for the self-cleavage assay, suggesting that both assays are investigating similar steps along the reaction pathway (*29*, *30*). This analysis revealed several positions within the VS RNA that are quite sensitive to modification. The majority of these nucleotides are located in helix II, helix VI (730 loop), the II−III−VI and III−IV−V helix junctions, and loop V, which forms a kissing interaction with loop I. All of these regions are known to make important contributions to formation of a functional RNA (*6*, *9*, *10*, *14*, *36*). Two consecutive bases in helix II, G653 and G654, show an interference pattern consistent with a possible role as receptor base pairs of two consecutive A-minor motifs.

Of all the positions in the VS ribozyme, A756 was the most sensitive to modification, showing either interference or enhancement with all seven of the adenosine nucleotide analogues used in this study. Many of these interferences correlate well with previously published mutational and kinetic studies of VS ribozymes that contained site-specific analogue substitutions at A756 (*11*, *13*). dA showed a 10-fold reduction in rate ($\kappa = 3$), while substitution of 2′-deoxy-Pur or 2′-deoxy-2AP reduced catalytic activity more than 1000-fold ($\kappa > 4$ for the ribose analogues) (*13*). Similarly, site-specific substitution of A756 with 2′-deoxy-DAP caused a 100-fold reduction in catalytic rate ($\kappa = 6$ for the ribose analogue), while 2′-deoxy-7dA showed slight enhancement compared to the single 2′-deoxy substitution ($\kappa = 0.4$ for the ribose analogue) (*13*). Thus, the data from these two independent experiments are qualitatively similar.

In addition to the base- and ribose-modified nucleotide analogues, a series of pK_a-shifted analogues were used to assess important ionization events in the VS ribozyme. The analogue n^8A had not been introduced into the VS RNA, nor have any of the analogues been analyzed as a function of pH, so the interference patterns at A756 and other residues within the ribozyme are of particular interest. Only one site within the entire VS RNA demonstrated an interference pattern consistent with base ionization, that at A756. The data in favor of this conclusion are as follows: (i) Incorporation at A756 of two analogues (n^8A or Pur) with a reduced

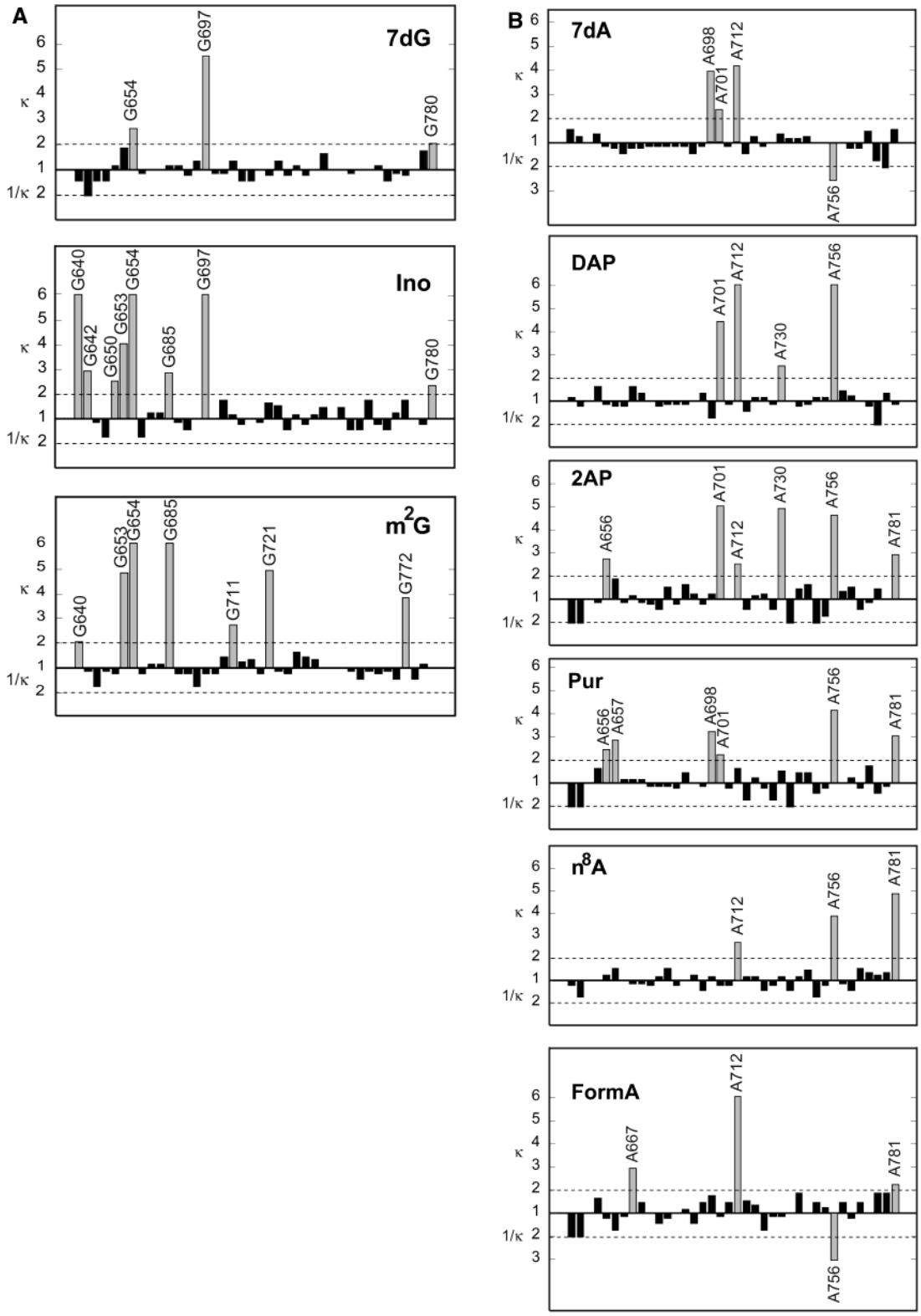

FIGURE 5: Quantitated interference (κ) values from modified guanosine (A) and adenosine (B) analogues at pH 7. Individual κ values for each analogue are plotted for each G or A residue in the VS sequence. The sequence reads from left to right (5′ to 3′). Sites of significant interferences ($\kappa > 2$) or enhancements ($\kappa < 0.5$) are indicated as a shaded gray bar with the sequence number indicated at the end of the bar. Filled black bars indicate positions in the sequence that were not significantly affected by the analogue substitution. κ values less than 1 are reported as $1/\kappa$, and the value is graphed below the center point.

pK_a interfered with activity. (ii) Substitution of two analogues with an elevated pK_a (FormA, 7dA) resulted in enhancement exclusively at A756. (iii) The interferences from n^8A and Pur could be almost fully rescued by reducing the reaction buffer to a slightly acidic pH. (iv) A756 interference from an analogue whose pK_a is not different from adenosine (dA) was not affected by the change in the reaction pH, and interferences at several other positions were stronger at the reduced pH. These, and previously published data, provide compelling evidence that the chemical identity of A756 is

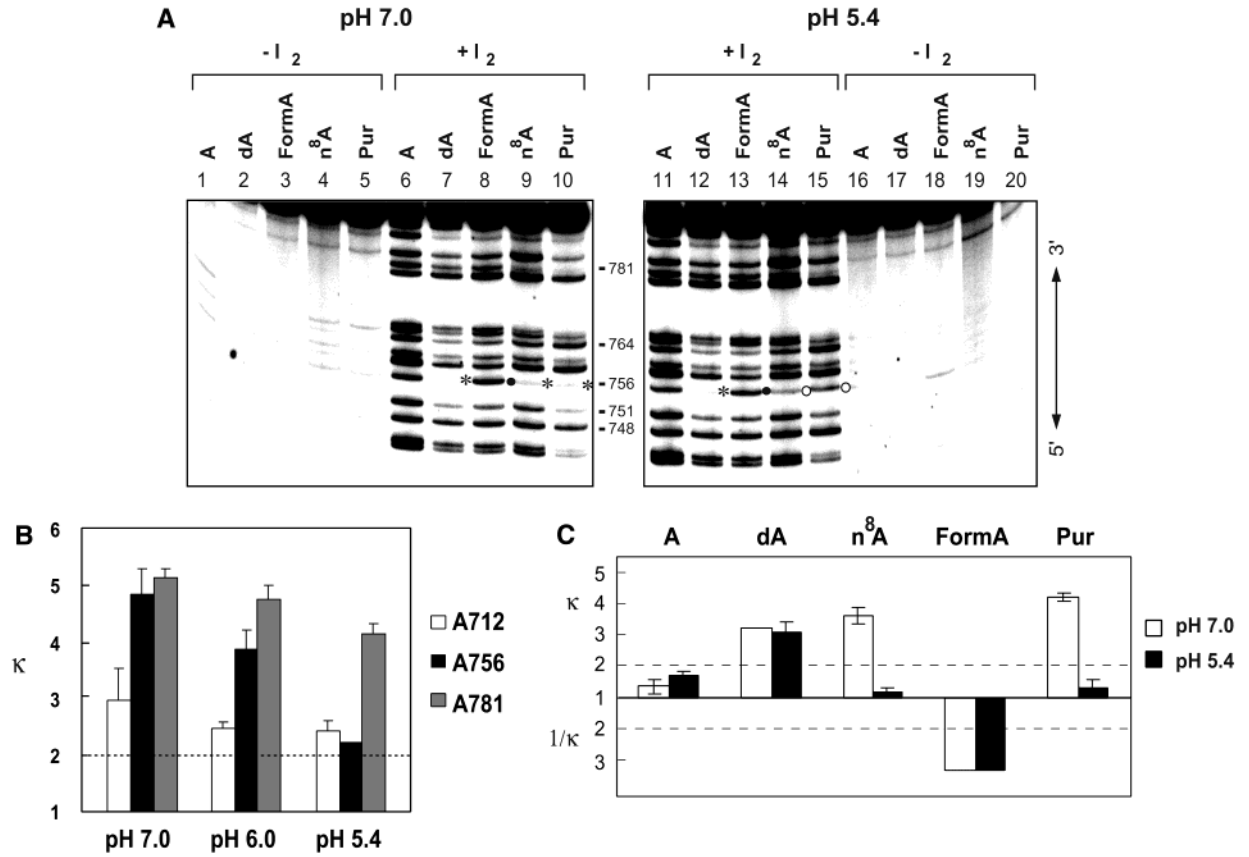

FIGURE 6: pH dependence of adenosine analogue interference. (A) Interference pattern at A756 with A, dA, Pur, n^8A, and FormA, compared at pH 7 and 5.4. The position of A756 is indicated to the left of the gel. Sites of analogue interference are indicated by an asterisk (∗), while sites of pH-dependent rescue are indicated by an open circle (○). Sites of enhancement are indicated with a closed circle (●). (B) Magnitude of n^8A interference at A712, A756, and A781 as a function of pH from 7.0 to 5.4. Black bars designate interference at A756, gray bars indicate A781, and open bars represent A712. Interference values were averaged from two experiments, and error bars indicate the deviation from the mean. (C) Interference at A756 for analogues A, dA, Pur, n^8A, and FormA, compared at pH 7.0 and 5.4. The κ values are the average of two experiments; error bars indicate deviation from the mean. κ values less than 1 are reported at $1/\kappa$, and the value is graphed below the center point.

important for VS ribozyme catalysis, with regard both to the array of functional groups that it presents in the active site and to its ability to become protonated at some point in the reaction pathway.

Ionization of A756 within the VS Active Site. If A756 is ionized, as suggested by these data, then how might protonation of this adenosine promote the reaction of the VS ribozyme? The two most likely possibilities can be broadly categorized into structural or catalytic effects. Protonated bases can participate in noncanonical base-pairing interactions that can stabilize secondary as well as tertiary interactions in RNA. For example, C^+•G Hoogsteen pairs and A^+•C wobble pairs are fairly common structural features in RNA molecules and utilize the additional proton as an ancillary functional group for hydrogen bonding (*37*, *38*). NMR analysis of A^+•C protonated wobble pairs indicate that the pK_a of the A is perturbed significantly toward neutrality (pH 5.0−6.0) (*39*). In domain B of the hairpin ribozyme, adenosine protonation is observed to stabilize base-stacking interactions in addition to hydrogen bond formation (*39*). Furthermore, the amino proton of adenosine becomes more acidic upon N1 protonation, enabling it to form stronger hydrogen bonds. It is thus possible that protonation of A756 may serve a structural role in VS RNA. For example, the imino proton of A756 may interact with nucleotides within the substrate helix in order to align the substrate within the active site of the RNA. However, this is unlikely, as mutating A756 does not affect substrate binding (*10*).

In addition to structural stabilization, protonated bases can also play direct roles in RNA catalysis. An ionizable nucleotidyl base could serve as a general acid or base in the phosphotransfer reaction, or the positive charge of the protonated adenosine could stabilize a developing negative charge of the transition state (*20*). For example, within the crystal structure of the hepatitis delta virus (HDV) ribozyme, a small nucleolytic RNA enzyme that performs a phosphotransfer reaction equivalent to that of the VS ribozyme, the critical cytidine residue, C75, is positioned in close proximity to the 5′-oxygen leaving group (*40*). Mutation of C75 to U abolishes catalytic activity, though activity can be partially restored by the addition of imidazole or other exogenous bases (*41*). Strong evidence for the role of C75 ionization in the HDV reaction mechanism was provided by Nakano et al., who showed that, under conditions of low divalent metal ion concentration, the pK_a of the HDV ribozyme reaction approaches neutrality, consistent with the apparent pK_a of 6.1 for residue C75 (*19*). Although NMR measurements on the product form of the ribozyme failed to detect an unusual pK_a for C75 (*42*), NAIM experiments with the pK_a-shifted cytidine analogues provided additional support for the expectation that ionization of the N3 of C75 is necessary for HDV activity (*22*). The current evidence

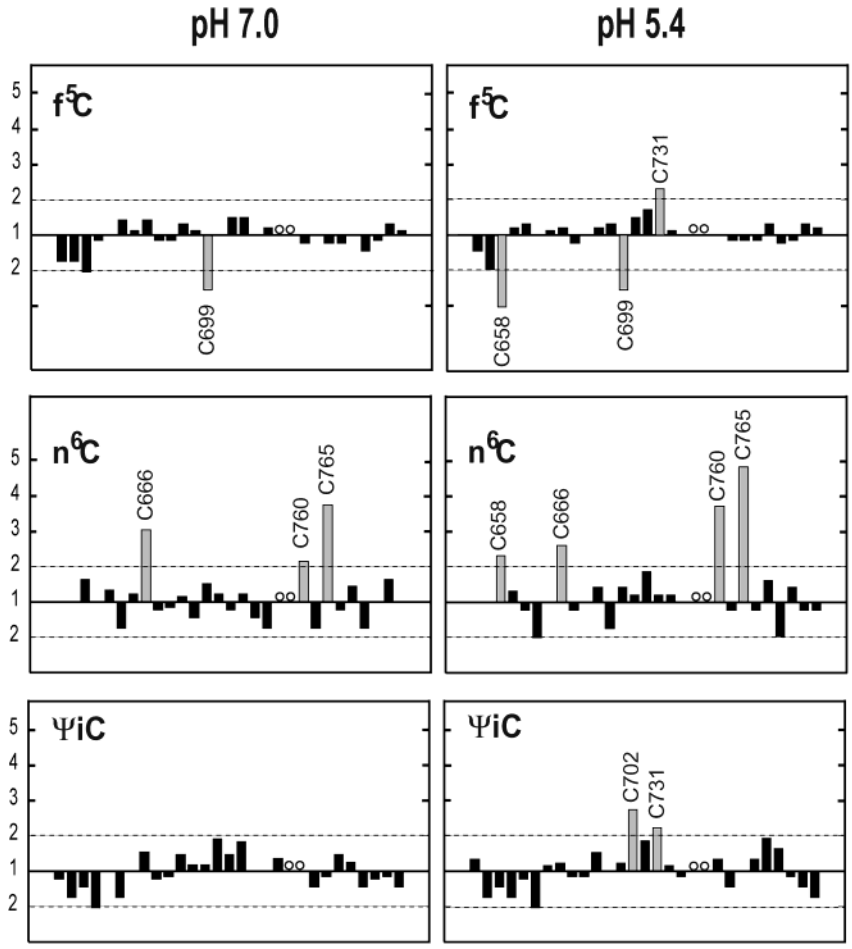

FIGURE 7: Interference analysis for the pK_a-shifted cytidine analogues at pH 5.4 and 7.0. The sequence reads 5′ to 3′ from left to right for each cytidine nucleotide in VS. Sites of significant interferences ($\kappa > 2$) or enhancements ($\kappa < 0.5$) are indicated in gray shading and with sequence number. Dark bars indicate positions in the sequence that were not significantly affected by the analogue substitution. The open circles indicate positions that were uninformative sites due to strong phosphorothioate effects. κ values less than 1 are reported at $1/\kappa$, and the value is graphed below the center point.

supports a model in which C75 acts as a general acid in the reaction to protonate and stabilize the 5′-oxyanion, while a metal hydroxide is implicated as the general base (*19*).

The hairpin ribozyme, another small self-cleaving RNA, might be the most relevant system in comparison to the VS enzyme. The recent crystal structure of a vanadate-complexed hairpin RNA provides our best view to date of a ribozyme transition state (*43*). This structure suggests that the N1 of A38 may have a perturbed pK_a, which would allow it to play a role in protonating the 5′-oxyanion leaving group during the cleavage reaction. Analysis of the hairpin ribozyme reaction with the series of adenosine analogues used in the current report supports the importance of A38, particularly a critical role for the exocyclic amine, while at the same time implicates A10 ionization as playing a functional role in a step following docking (*18*, *44*).

There are several lines of evidence that suggest that A756 protonation plays a catalytic, rather than a structural, role in the VS reaction. First, mutation of A756 to any other base results in drastic reductions in self-cleavage activity (*10*, *11*), but structural comparison of wild-type and mutant VS constructs by FRET indicates that mutation of A756 does not affect the global folding of the VS RNA (*14*). Second, A756 variants bind substrate efficiently (*14*). Third, although attempts to rescue activity of an A756 abasic site with imidazole were unsuccessful, an experiment that provided evidence for C75 ionization in the HDV ribozyme, the VS results are inconclusive (*13*). Exogenous adenosine base was also unable to rescue the abasic mutation, suggesting that introduction of the abasic site may have altered the local structure of the 730 loop, preventing access of the base. Fourth, 4-thioU cross-linking experiments pinpoint A756 as being in close proximity to the cleavage site (*15*). Fifth, a FRET-derived structural model of the VS ribozyme generated by Lilley and co-workers places A756 near the substrate helix, where it can make significant tertiary interactions with nucleotides at the cleavage site (*14*). At the very least, these studies place A756 in a position for it to serve a catalytic function. Evidence of base ionization makes A756 an ideal candidate for a role in charge neutralization of the transition state and/or a role in proton transfer. By analogy to the predicted roles of hairpin A38 or HDV C75, the N1 of A756 could serve as a general base to activate the 5′-OH or as a general acid to protonate the leaving 2′-oxyanion during the ligation reaction.

If A756 is protonated at some point in the reaction profile, is the pK_a of A756 by necessity perturbed? It is well established that RNA nucleosides do not have functional groups with near neutral pK_as. The N1 and N3 groups of adenosine and cytidine have potential for protonation, though

their pK_as are too acidic to be significantly protonated at physiological pH (*38*). The pK_as increase by about half a pH unit when the 5′- and 3′-hydroxyls are phosphorylated, as is the case in an RNA polymer, but the pK_as remain too low to have much effect on a reaction proceeding efficiently at neutral pH (*39*). However, RNAs, like proteins, can fold into tertiary structures and create microenvironments that lead to local pK_a perturbations of the bases. Thus, a strong, albeit indirect, prediction stemming from the current data is that if A756 ionization plays a meaningful role in the VS reaction, then the pK_a of A756 must be perturbed at some point in the reaction profile. If this perturbation occurs primarily in the transition state, which is certainly possible, then it may be difficult to detect by NMR or other steady-state methods. On the basis of the principle of microscopic reversibility, if A756 plays a role as a general base (for example) in this concerted ligation reaction, then it must also function as a general acid during cleavage. Unless the pK_a of the base were shifted toward neutrality, it could not make a meaningful contribution to the reaction, and its ionization would have gone undetected in our assay. We cannot ascertain from the NAIM data how much the A756 pK_a is perturbed, but the interference rescue at pH 5.4 appears to place 5.4 as a lower limit. In the HDV ribozyme, the N4 amino group of C75 participates in hydrogen bonding to the R_P oxygen of C22, an interaction that has been hypothesized to be important for perturbing the pK_a of C75 (*19*, *40*). However, under acidic conditions we observed Pur interference rescue at A756, arguing that the perturbation of the pK_a of A756 may not occur via electron donation to the purine ring via the N6 amino group.

RNA catalyses in small nucleolytic RNAs, such as the VS ribozyme, serve as model systems for understanding catalysis by the peptidyl transferase center of the ribosome, which is also a ribozyme (*45*, *46*). The complexity of assigning a particular functional role to an ionized base is evident from studies completed on that system. In that case there is both a high-resolution crystal structure and kinetic evidence implicating a single ionizable group within the peptidyl transferase center as critical for activity (*46*, *47*). Yet, the role and identity of this ionizable group remains in doubt. It is possible that the active site residue in the ribosome, A2451, acts as a general acid or general base to catalyze the transacylation reaction, but it is also possible that deprotonation of the neighboring A2450, which appears to be protonated in an A^+·C wobble pair, induces a conformational change in the active site (*47*, *48*). Similar complexity may exist for A756 in the VS ribozyme, but the present data provide fairly compelling evidence that ionization of this residue is functionally important. The exact role it plays in ribozyme function awaits further analysis.

ACKNOWLEDGMENT

We thank Adegboyega Oyelere for the synthesis of the nucleotide analogues used in this study. We also thank Sean Ryder, Ashley Eversole, and Mark Parnell for comments regarding the manuscript.

REFERENCES

1. Griffiths, A. J. F. (1995) Natural plasmids of filamentous fungi, *Microbiol. Rev. 59*, 673−685.
2. Saville, B. J., and Collins, R. A. (1990) A site-specific self-cleavage reaction performed by a novel RNA in *Neurospora* mitochondria, *Cell 61*, 685−696.
3. Guo, H. C., De Abreu, D. M., Tillier, E. R., Saville, B. J., Olive, J. E., and Collins, R. A. (1993) Nucleotide sequence requirements for self-cleavage of *Neurospora* VS RNA, *J. Mol. Biol. 232*, 351−361.
4. Jones, F. D., Ryder, S. P., and Strobel, S. A. (2001) An efficient ligation reaction promoted by a Varkud Satellite ribozyme with extended 5′- and 3′-termini, *Nucleic Acids Res. 29*, 5115−5120.
5. Anderson, A. A., and Collins, R. A. (2001) Intramolecular secondary structure rearrangement by the kissing interaction of the *Neurospora* VS ribozyme, *Proc. Natl. Acad. Sci. U.S.A. 98*, 7730−7735.
6. Rastogi, T., Beattie, T. L., Olive, J. E., and Collins, R. A. (1996) A long-range pseudoknot is required for activity of the *Neurospora* VS ribozyme, *EMBO J. 18*, 2820−2825.
7. Andersen, A. A., and Collins, R. A. (2000) Rearrangement of a stable RNA secondary structure during VS ribozyme catalysis, *Mol. Cell 5*, 469−478.
8. Flinders, J., and Dieckmann, T. (2001) A pH controlled conformational switch in the cleavage site of the VS ribozyme substrate RNA, *J. Mol. Biol. 308*, 665−679.
9. Beattie, T. L., and Collins, R. A. (1997) Identification of functional domains in the self-cleaving *Neurospora* VS ribozyme using damage selection, *J. Mol. Biol. 267*, 830−840.
10. Lafontaine, D. A., Wilson, T. J., Norman, D. G., and Lilley, D. M. J. (2001) The A730 loop is an important component of the active site of the VS ribozyme, *J. Mol. Biol. 312*, 663−674.
11. Sood, V. D., and Collins, R. A. (2002) Identification of the catalytic subdomain of the VS ribozyme and evidence for remarkable sequence tolerance in the active site loop, *J. Mol. Biol. 320*, 443−454.
12. Rastogi, T., and Collins, R. A. (1998) Smaller, faster ribozymes reveal the catalytic core of *Neurospora* VS RNA, *J. Mol. Biol. 277*, 215−224.
13. Lafontaine, D. A., Wilson, T. J., Zhao, Z., and Lilley, D. M. J. (2002) Functional group requirements in the probable active site of the VS ribozyme, *J. Mol. Biol. 323*, 23−34.
14. Lafontaine, D. A., Norman, D. G., and Lilley, D. M. J. (2002) The global structure of the VS ribozyme, *EMBO J. 21*, 2461−2471.
15. Hiley, S. L., Sood, V. D., Fan, J., and Collins, R. A. (2002) 4-thio-U cross-linking identifies the active site of the VS ribozyme, *EMBO J. 21*, 4691−4698.
16. Murray, J. B., Seyhan, A. A., Walter, N. G., Burke, J. M., and Scott, W. G. (1998) The hammerhead, hairpin and VS ribozymes are catalytically proficient in monovalent cations alone, *Chem. Biol. 5*, 587−595.
17. Collins, R. A., and Olive, J. E. (1993) Reaction conditions and kinetics of self-cleavage of a ribozyme derived from *Neurospora* VS RNA, *Biochemistry 32*, 2795−2799.
18. Ryder, S. P., Oyelere, A. K., Padilla, J. L., Klostermeier, D., Millar, D. P., and Strobel, S. A. (2001) Investigation of adenosine base ionization in the hairpin ribozyme by nucleotide analogue interference mapping, *RNA 7*, 1454−1463.
19. Nakano, S., Chadalavada, D. M., and Bevilacqua, P. C. (2000) General acid−base catalysis in the mechanism of a hepatitis delta virus ribozyme, *Science 287*, 1493−1497.
20. DeRose, V. J. (2002) Two decades of RNA catalysis, *Chem. Biol. 9*, 961−969.
21. Oyelere, A. K., and Strobel, S. A. (2000) Biochemical detection of cytidine protonation within RNA, *J. Am. Chem. Soc. 122*, 10259−10267.
22. Oyelere, A. K., Kardon, J. R., and Strobel, S. A. (2002) pK_a perturbation in genomic hepatitis delta virus ribozyme catalysis evidence by nucleotide analogue interference mapping, *Biochemistry 41*, 3667−3675.
23. Wierzchowski, J., Wielgus-Kutrowska, B., and Shugar, D. (1996) Fluorescence emission properties of 8-azapurines and their nucleosides, and application to the kinetics of the reverse synthethic reaction of purine nucleoside phosphorylase, *Biochim. Biophys. Acta 1290*, 9−17.
24. Kierdaszukm, B., Modrak-Wojcik, A., Wierzchowski, J., and Shuga, D. (2000) Formycin A and its N-methyl analogues, specific inhibitors of *E. coli* purine nucleoside phosphorylase (PNP): Induced tautomeric shifts on binding to enzyme, and enzyme-

ligand fluorescence resonance energy transfer, *Biochim. Biophys. Acta 1476*, 109−128.
25. Fasman, G. D. (1975) in *Handbook of biochemistry and molecular biology* (Fasman, G. D., Ed.) CRC Press, Cleveland, OH.
26. Szewczak, A. A., Orteleva-Donnelly, L., Zivarts, M. V., Oyelere, A. K., Kazantsev, A. V., and Strobel, S. A. (1999) An important base triple anchors the substrate helix recognition surface within the *Tetrahymena* ribozyme active site, *Proc. Natl. Acad. Sci. U.S.A. 96*, 11183−11188.
27. Orteleva-Donnelly, L., Szewczak, A. A., Gutell, R. R., and Strobel, S. A. (1998) The chemical basis of adenosine conservation throughout the *Tetrahymena* ribozyme, *RNA 4*, 498−519.
28. Ryder, S. P., and Strobel, S. A. (1999) Nucleotide analog interference mapping, *Methods 18*, 38−50.
29. Sood, V. D., Beattie, T. B., and Collins, R. A. (1998) Identification of phosphate groups involved in metal binding and tertiary interactions in the core of the *Neurospora* VS Ribozyme, *J. Mol. Biol. 282*, 741−750.
30. Sood, V. D., Yekta, S., and Collins, R. A. (2002) The contribution of the 2′-hydroxyls to the cleavage activity of the *Neurospora* VS ribozyme, *Nucleic Acids Res. 30*, 1132−1138.
31. Strobel, S. A., and Shetty, K. (1997) Defining the chemical groups essential for *Tetrahymena* group I intron function by nucleotide analog interference mapping, *Proc. Natl. Acad. Sci. U.S.A. 94*, 2903−2908.
32. Rife, J. P., Cheng, C. S., Moore, P. B., and Strobel, S. A. (1998) The synthesis of RNA containing the modified nucleotides N-2-methylguanosine and N-6,N-6-dimethyladenosine, *Nucleosides Nucleotides 17*, 2281−2288.
33. Orteleva-Donnelly, L., Kronman, M., and Strobel, S. A. (1998) Identifying RNA minor groove tertiary contacts by nucleotide analog interference mapping with N^2-Methylguanosine, *Biochemistry 37*, 12933−12942.
34. Nissen, P., Ippolita, J. A., Ban, N., Moore, P. B., and Steitz, T. A. (2001) RNA tertiary interactions in the large ribosomal subunit: The A-minor motif, *Proc. Natl. Acad. Sci. U.S.A. 98*, 4899−4903.
35. Soukup, J. K., Minakawa, N., Matsuda, A., and Strobel, S. A. (2002) Identification of A-minor tertiary interactions within a bacterial group I intron active site by 3-deazaadenosine interference mapping, *Biochemistry 41*, 10426−10438.
36. Lafontaine, D. A., Norman, D. G., and Lilley, D. M. J. (2001) Structure, folding and activity of the VS ribozyme: importance of the 2-3-6 helical junction, *EMBO J. 20*, 1415−1424.
37. Cai, Z., and Tinoco, I. (1996) Solution structure of loop A from the hairpin ribozyme from tobacco ringspot virus satellite, *Biochemistry 35*, 6026−6036.
38. Saenger, W. (1984) in *Principles of Nucleic Acid Structure*, Springer-Verlag, New York.
39. Ravindranathan, S., Butcher, S. E., and Feigon, J. (2000) Adenine protonation in domain B of the hairpin ribozyme, *Biochemistry 39*, 16026−16032.
40. Ferre-D'Amare, A. R., Zhou, K., and Doudna, J. A. (1998) Crystal structure of a hepatitis delta virus ribozyme, *Nature 395*, 567−574.
41. Perrotta, A. T., Shih, I., and Been, M. D. (1999) Imidazole rescue of a cytosine mutation in a self-cleaving ribozyme, *Science 286*, 123−126.
42. Luptack, A., Ferre-D'Amare, A. R., Kaihong, Z., Zilm, K. W., and Doudna, J. A. (2001) Direct pK_a measurement of the active site cytosine in a genomic hepatitis delta virus ribozyme, *J. Am. Chem. Soc. 123*, 8447−8452.
43. Rupert, P. B., Massey, A. P., Sigurdsson, S. T., and Ferre-D'Amare, A. R. (2002) Transition state stabilization by a catalytic RNA, *Science 298*, 1421−1424.
44. Ryder, S. P., and Strobel, S. A. (1999) Nucleotide analog interference mapping the hairpin ribozyme: Implications for secondary and tertiary structure formation, *J. Mol. Biol. 291*, 295−311.
45. Nissen, P., Hansen, J., Ban, N., Moore, P. B., and Steitz, T. A. (2000) The structural basis of ribosome activity in peptide bond formation, *Science 289*, 920−930.
46. Ban, N., Nissen, P., Hansen, J., Moore, P. B., and Steitz, T. A. (2000) The complete atomic structure of the large ribosomal subunit at 2.4 A resolution, *Science 289*, 905−920.
47. Katunin, V. I., Muth, G. W., Strobel, S. A., Wintermeyer, W., and Rodnina, M. V. (2002) Important contribution to catalysis of peptide bond formation by a single ionizing group within the ribosome, *Mol. Cell 10*, 339−346.
48. Muth, G. W., Chen, L., Kosek, A. B., and Strobel, S. A. (2001) pH-dependent conformational flexibility within the ribosomal petidyl transferase center, *RNA 7*, 1403−1415.

BI020707T